Supporting Information

Chang et al. 10.1073/pnas.1113770109

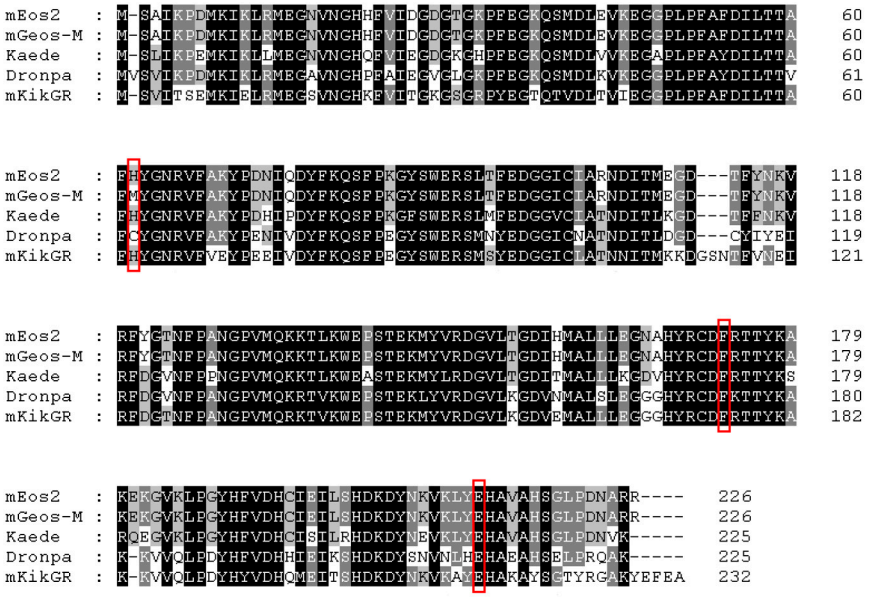

Fig. S1. Sequence alignment of mEos2, mGeos-M, Kaede, Dronpa, and mKikGR. Mutations from mEos2 to mGeos-M and other mGeos are marked by a red frame. F173S (mEos2 amino acid sequence) mutants demonstrated faster off-switching kinetics, similar to those of rsFastLime (Dronpa-Val157Gly).

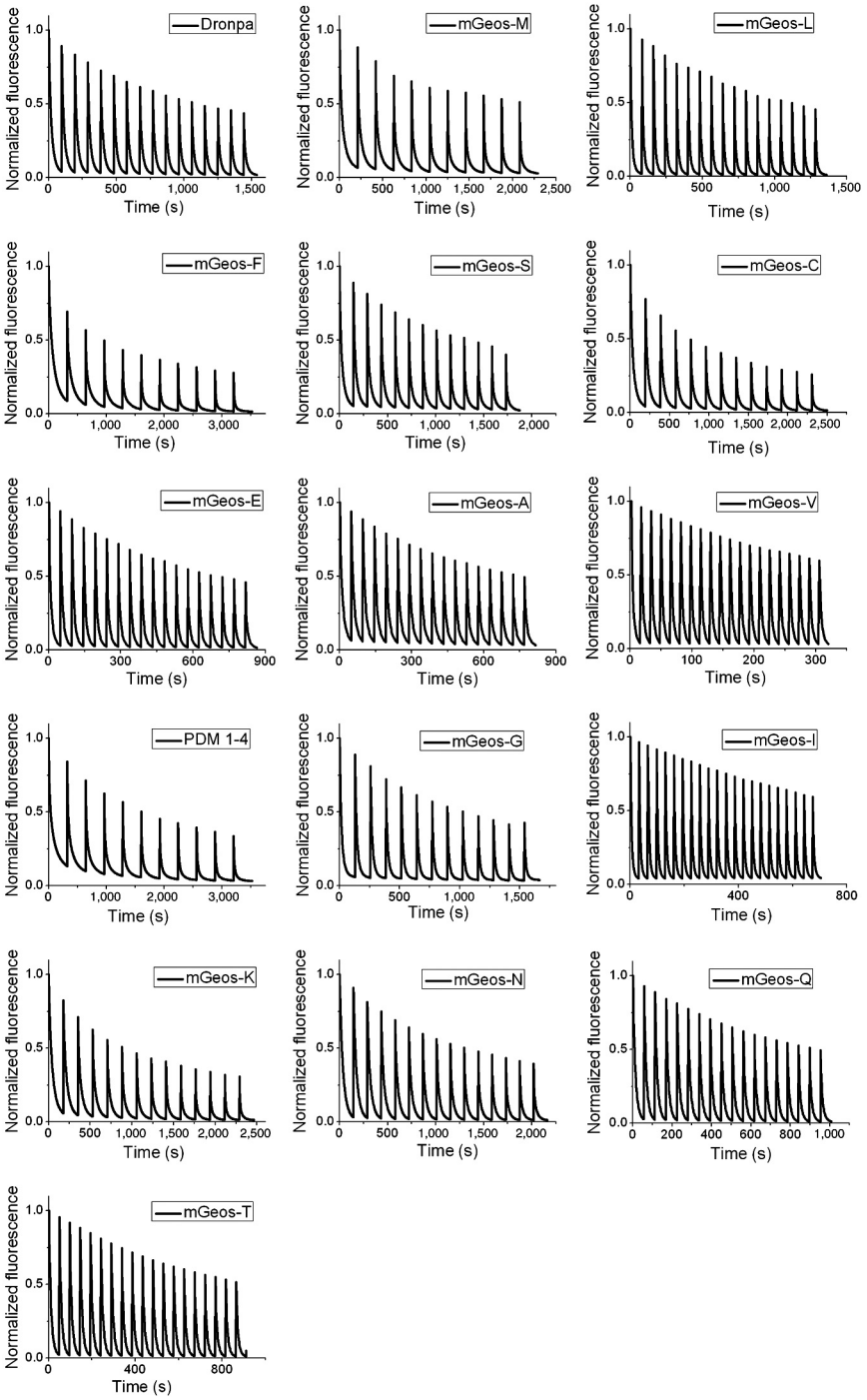

Fig. S2. Photoswitching characteristics of Dronpa and mGeos-X. Photoswitching kinetics of the fluorescence was recorded by laser scanning confocal microscope on HeLa cells expressing Dronpa and mGeos-X. During the entire experiments, the 405 nm and 488 nm laser power, scanning speed, gain (set at 2.5), amplification and off-set value were held constant.

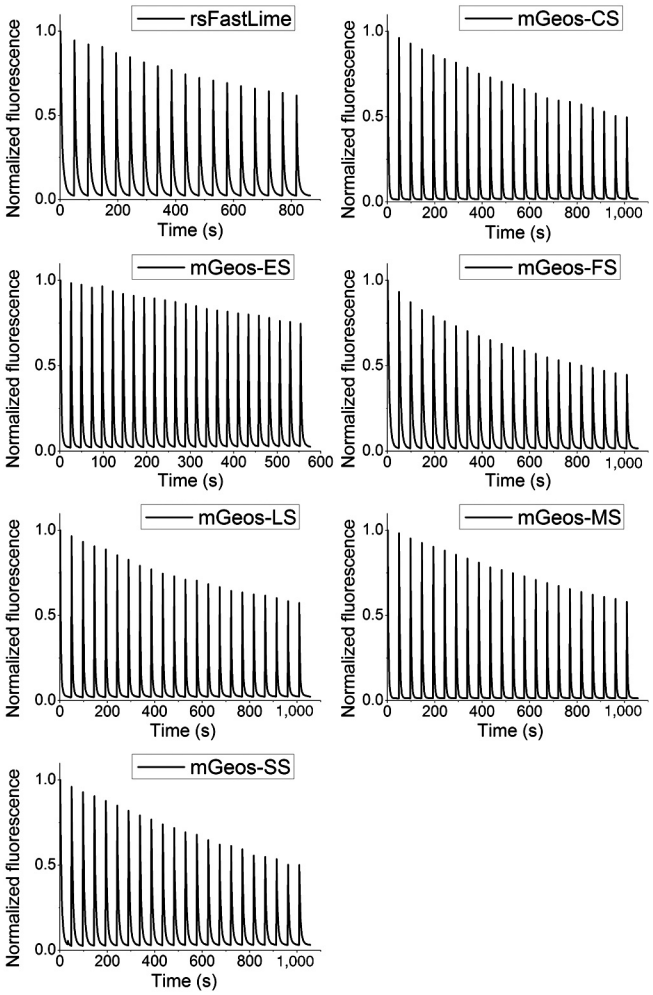

Fig. S3. Photoswitching characteristics of mGeos-XS and rsFastLime. Photoswitching kinetics of the fluorescence was recorded by laser scanning confocal microscope on HeLa cells expressing rsFastLime and mGeos-XS. During the entire experiments, the 405 nm and 488 nm laser power, scanning speed, gain (set at 2.5), amplification and off-set value were held constant.

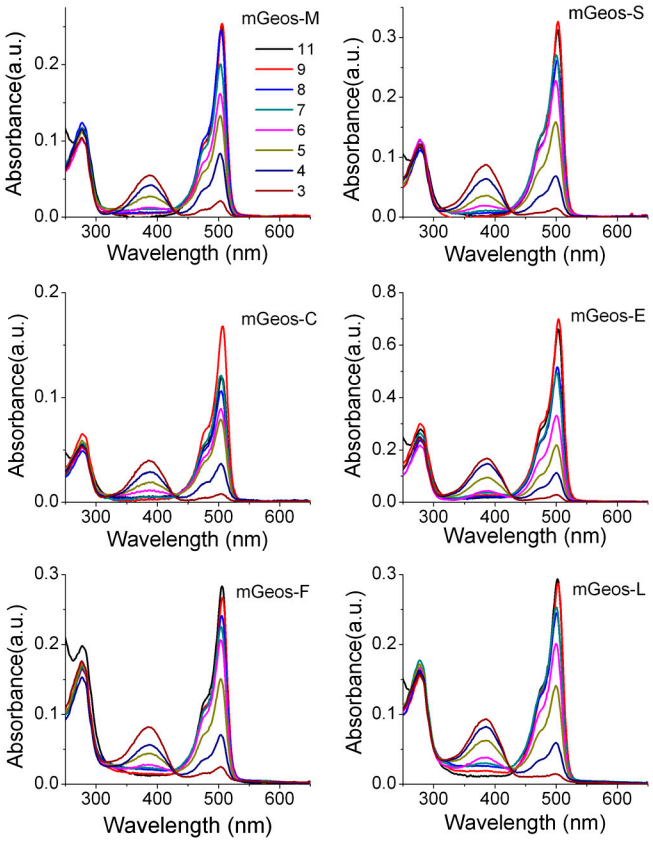

Fig. S4. Equilibrium pH dependence of the mGeos absorbance spectra. mEos2 H62 mutants show different pK_a values. mGeos-E and mGeos-C were more acid-sensitive, similar to the red photoswitchable proteins mApple and rsTagRFP, whereas mGeos-M showed a better pH stability than that of Dronpa.

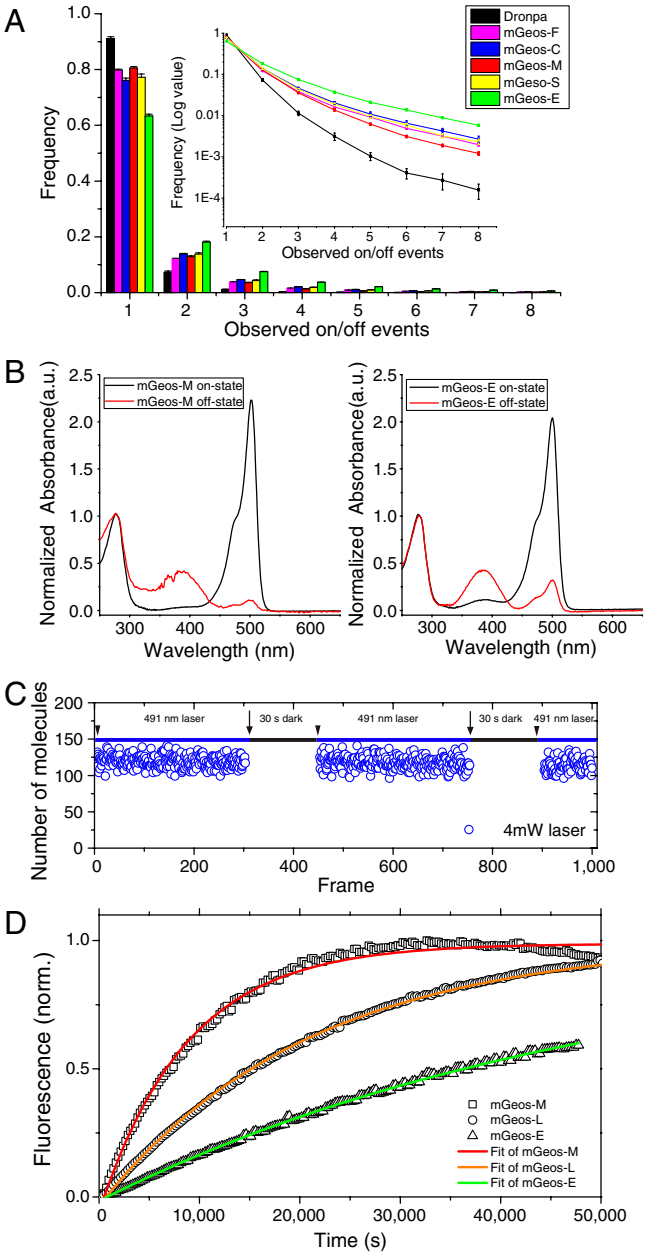

Fig. S5. mGeos-E exhibits more on/off events than other mGeos. (*A*) Histogram of observed on/off switching (or blinking) events for purified biotin-conjugated Dronpa and mGeos immobilized to streptavidin-conjugated coverslip during the same time lapse. The molecules that were turned on by 491 nm laser were counted. Number of on events is calculated as the number of localizations within an interlocalization spacing of 30 nm (approximately 2-fold of average position error). (*B*) Absorption spectra of purified mGeos-M and mGeos-E in on-state and off-state. Please note that there is a high absorbance at 491 nm in the off-state of mGoes-E. (*C*) It was reported that some fluorescent proteins such as Dronpa-M159T (relaxation half-time: 0.5 min) (1) and mApple (almost complete recover in 0.5 min) (2) could relax quickly in the darkness from their temporarily dark-state back to fluorescence. To test whether the spontaneous recovery contribute to the single molecular detection of mGoes-E when using the 491 nm laser alone, we shut down the laser as indicated by the arrows for 30 s. If there is a fast relaxing process, more single molecules would be accumulated and collected at the time point when the laser was turned on again as indicated by arrow heads. However, there was no significant difference between the numbers of the collected single molecules before and after the laser break, suggesting that there was little contribution of spontaneous recovery during the single molecular imaging of mGoes-E. (*D*) Spontaneous recovery curves of purified mGeos-M/E/L from off-state. Curves were normalized to the amplitudes of fitted exponentials. Please see the rates of spontaneous recovery of other mGeos in Table 1.

1. Stiel AC, et al. (2007) 1.8 A bright-state structure of the reversibly switchable fluorescent protein Dronpa guides the generation of fast switching variants. *Biochem J* 402:35–42.
2. Shaner NC, et al. (2008) Improving the photostability of bright monomeric orange and red fluorescent proteins. *Nat Methods* 5:545–551.

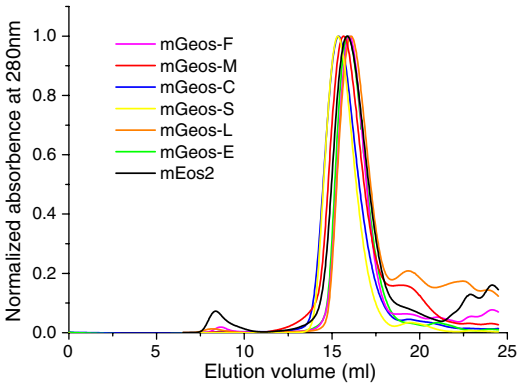

Fig. S6. Gel filtration analysis of mGeos and mEos2. Size exclusion chromatography of mGeos and mEos2 (approximate 3–4 mg $*$ mL^{-1}) in PBS using a Superdex 200 10/300 GL column. The elution volume of mGeos and mEos2 are nearly the same, indicating that their oligomeric states are identical.

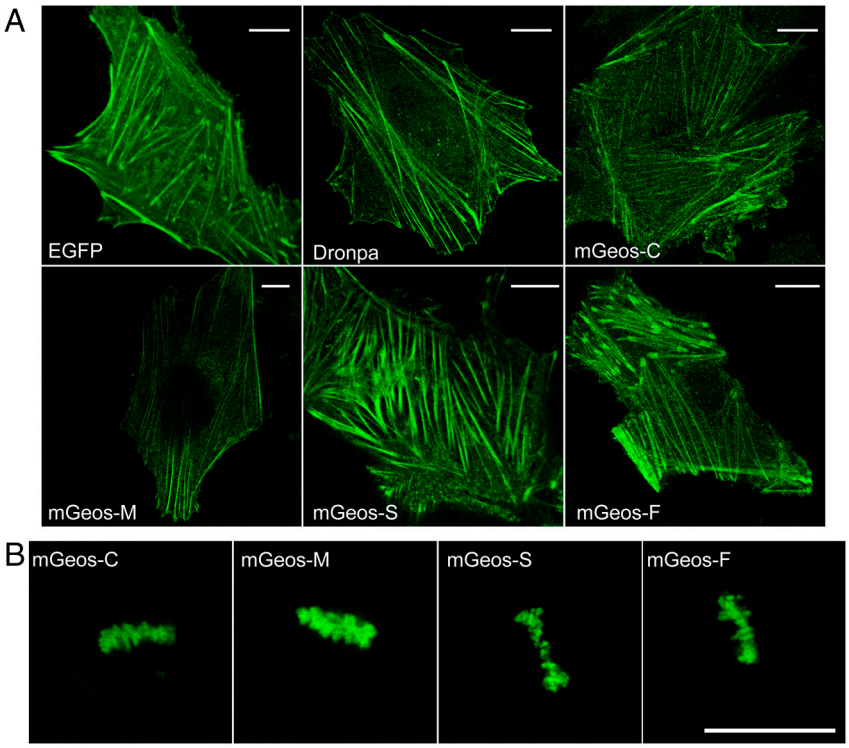

Fig. S7. HeLa cells expressing mGeos fusion proteins. HeLa cells expressing EGFP-β-actin, Dronpa-β-actin, PDM 1–4-β-actin, and three kinds of mGeos-β-actin show similar localization (*A*). Confocal images of HeLa cells expressing mGeos-histone H2B (human) in mitotic phase (*B*). Scale bars: 10 μm.

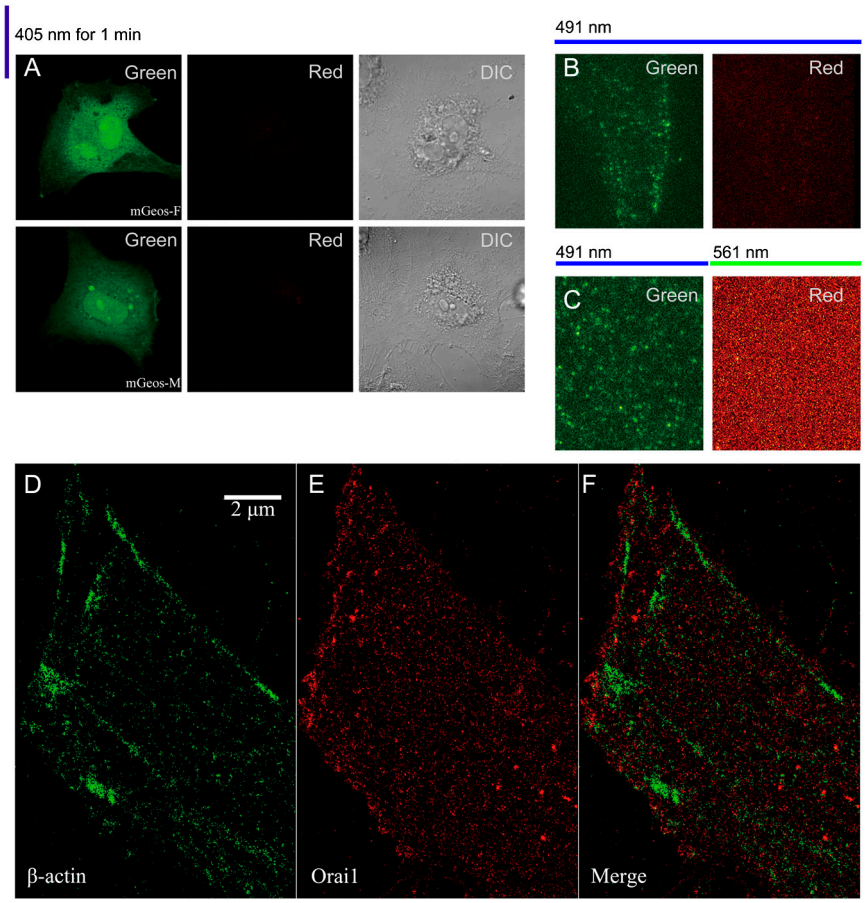

Fig. S8. Dual-channel crosstalk experiments of mGeos-M and PAmCherry1. (*A*) Confocal images of mGeos-F and mGeos-M in both red and green channels after strong 405 nm laser exposure for 1 min. In this situation, mEos2 has been largely converted from green form to red one. However, there is still no signal in red channel for both mGeos-F and mGeos-M. (*B*) In vivo images of mGeos-M-β-actin expressing cell. There are no red form single molecules excited in 491 nm laser, confirming no crosstalk between mGeos-M and other red photoactive or photo-switching fluorescent proteins or dyes. We also tested mGeos-F and mGeos-S and both of them show the same feature as mGeos-M. (*C*) In vitro images of purified mGeos-F protein on glass excited under 491 nm or 561 nm laser. Single molecule signals were observed in green channel when excited by 491 nm laser, but were not seen in red channel when excited by 561 nm laser alone or combined with 405 nm laser, suggesting no photoconversion of mGeos-F to red form. We also tested mGeos-M and mGeos-S and both of them show the same feature as mGeos-F. (*D*–*F*) PALM images of an HeLa cell coexpressed with mGeos-M-β-actin and Orai1-PAmCherry1. Orai1 is a transmembrane channel protein localized to the plasma membrane, thus should have a different localization from β-actin. Indeed, merge image (*F*) shows nearly no overlap between the two proteins. Scale bars: 2 μm.

Table S1. Characteristics of mEos2 His62 mutants and mEos2 His62&F173S double mutants

				Slow mGeos		
H62X	Fluorescent protein	Bleaching per cycle	Off-state fluorescence	488 switching half-time	Normalized off-switching half-time compared with Dronpa	Description of mEos2 His62 mutations
	Dronpa	6.10%	4.20%	13.84	100%	ps*
	PDM1-4	10.25%	10.59%	36.14	261%	ps
A	mGeos-A	4.86%	6.42%	8.30	60%	ps
C	mGeos-C	11.52%	5.02%	23.91	173%	ps
D	mGeos-D	——	——	——	——	No fluorescence
E	mGeos-E	4.94%	3.17%	6.61	48%	ps
F	mGeos-F	11.63%	7.19%	52.28	378%	ps
G	mGeos-G	7.76%	7.11%	12.76	92%	ps
H	mEos2	——	——	——	——	pc†
I	mGeos-I	2.54%	4.81%	4.57	33%	ps
K	mGeos-K	9.66%	5.07%	29.52	213%	ps
L	mGeos-L	5.28%	1.90%	7.43	54%	ps
M	mGeos-M	6.38%	6.28%	21.03	152%	ps
N	mGeos-N	7.10%	3.07%	23.33	169%	ps
P	mGeos-P	——	——	——	——	No fluorescence
Q	mGeos-Q	4.60%	2.59%	8.83	64%	ps
R	mGeos-R	——	——	——	——	No fluorescence
S	mGeos-S	6.97%	5.94%	15.65	113%	ps
T	mGeos-T	4.01%	2.30%	7.95	57%	ps
V	mGeos-V	2.94%	4.25%	3.75	27%	ps
W	mGeos-W	——	——	——	——	No fluorescence
Y	mGeos-Y	——	——	——	——	No fluorescence
				Fast mGeos		
H62XF173S	Fluorescent protein	Bleaching per cycle	Off-state fluorescence	488 switching half-time	Normalized off-switching half-time compared with rsFastLime	Description of mEos2 His62&F173S mutations
	rsFastLime	2.79%	3.10%	14.83	100%	ps
CS	mGeos-CS	3.27%	2.54%	7.24	49%	ps
ES	mGeos-ES	1.26%	3.05%	4.96	33%	ps
FS	mGeos-FS	3.75%	2.80%	13.32	90%	ps
LS	mGeos-LS	2.60%	3.13%	6.48	44%	ps
MS	mGeos-MS	2.56%	1.91%	8.00	54%	ps
SS	mGeos-SS	3.23%	4.45%	11.80	80%	ps

*ps means photoswitchable;
†pc means photoconversion.

Table S2. Photon statistics for purified mGeos in vitro and β-actin linked mGeos in HeLa cells

		Total photon burst per molecule			Background photon per molecule	
		n	Mean	Median	Mean	Median
Purified mGeos*	mGeos-F	186,186	572.9071	450.4789	3.8630	3.6335
	mGeos-C	381,035	539.1392	466.0933	3.9077	3.6663
	mGeos-M	334,956	590.3668	491.9605	4.3183	3.9852
	mGeos-S	269,545	477.0508	415.0571	3.5798	3.3514
	mGeos-E	630,198	460.7853	425.9008	4.0704	3.9058
	mGeos-L	552,559	424.9025	388.1176	3.7294	3.5689
β-actin linked mGeos	mGeos-F	1,642,556	375.497	282.49	5.4088	5.2202
	mGeos-C	1,465,352	309.1058	255.242	5.0235	4.8154
	mGeos-M	1,878,091	459.0682	361.7952	6.8841	6.3330
	mGeos-S	2,514,005	396.8448	327.1493	6.2131	5.8846
	Dronpa	1,880,667	270.2028	227.8501	4.4372	4.2501
	PDM1-4	1,036,338	341.9071	294.4645	5.6584	5.4320
	mGeos-N	2,453,143	334.6510	283.9575	5.3985	5.1416
	mGeos-K	1,507,560	345.8167	288.3660	5.6158	5.4464

*buffer condition: PBS (pH = 7.4).